

Heavy Ions: Results from the Large Hadron Collider

TAPAN K. NAYAK^{a, *}

^aVariable Energy Cyclotron Centre, Kolkata - 700064, India

Abstract.

On November 8, 2010 the Large Hadron Collider (LHC) at CERN collided first stable beams of heavy ions (Pb on Pb) at center-of-mass energy of 2.76 TeV/nucleon. The LHC worked exceedingly well during its one month of operation with heavy ions, delivering about $10\mu\text{b}^{-1}$ of data, with peak luminosity reaching to $L_0 = 2 \times 10^{25}\text{cm}^{-2}\text{s}^{-1}$ towards the end of the run. Three experiments, ALICE, ATLAS and CMS, recorded their first heavy ion data, which were analyzed in a record time. The results of the multiplicity, flow, fluctuations, and Bose-Einstein correlations indicate that the fireball formed in nuclear collisions at the LHC is hotter, lives longer, and expands to a larger size at freeze-out as compared to lower energies. We give an overview of these as well as new results on quarkonia and heavy flavour suppression, and jet energy loss.

Keywords. Quark Gluon Plasma, fluctuations, flow, heavy flavour, quarkonia, jets, energy loss

PACS Nos. 12.38.Mh, 25.75.-q, 25.75.Dw, 25.75.Cj

1. Introduction

The Large hadron Collider (LHC) at CERN is the world's largest and highest energy accelerator, designed to address some of the most fundamental questions of recent times such as, whether Higgs particle exist or not, why laws of physics are not symmetrical between matter and anti-matter, what makes up the mysterious dark matter, and how do we understand the primordial state of matter after the Big Bang and before the formation of nucleons. The answers to each of these questions may not come that easy and may open up newer avenues in our quest to discover the mysteries of our Universe. The approach at LHC has been to address these issues by studying the particles produced in proton-proton (p-p) as well as ion-ion (such as Pb-Pb) collisions at extremely high energies. With the heavy ion collisions, the aim is to study the primordial state of matter consisting of quarks and gluons and verify the predictions of the Standard Model in conjunction with quantum chromodynamics (QCD).

Asymptotic freedom is a feature of QCD which states that at short distances the interaction between quarks becomes very weak, and as a result they behave like free particles. As we try to increase the distance between pairs of quarks, they will have more affinity for each other and hence will be interacting even more strongly with each other. So, it is almost impossible to isolate a free quark. It has been postulated that the early Universe,

*Tapan.Nayak@cern.ch

immediately after the Big Bang, consisted of asymptotically free quarks and gluons. Statistical QCD calculations predict that at high temperature and/or energy density a system of strongly interacting particles, consisting of quarks and gluons, is formed where the particles would interact fairly weakly due to asymptotic freedom. Such a phase consisting of (almost) free quarks and gluons is termed as the quark gluon plasma (QGP) [1, 2]. By colliding two relativistically accelerated heavy ions, it is possible to compress and heat the nuclei to such an extent that their individual protons and neutrons overlap, creating a region of enormously high energy density, where a relatively large number of free quarks and gluons can exist for a brief time. The experimental search for QGP began in the eighties with several fixed target experiments at Brookhaven National Laboratory (BNL) and CERN. The results from the experiments at Super Proton Synchrotron (SPS) led CERN to announce the evidence for a new state of matter in the year 2000. In the same year, the Relativistic Heavy Ion Collider (RHIC), a dedicated machine for QGP search became operational at BNL. The results of last decade of data taking at RHIC points to the creation of a new form of matter that behaves like a strongly interacting near perfect liquid. LHC, with an increase of energy by more than an order of magnitude compared to RHIC, provides an enormous opportunity to explore the new state of matter in great detail.

At the LHC, the first successful proton-proton (p-p) collisions took place in 2009, and a year later in November 2010, first collisions of Pb-Pb ions were established at $\sqrt{s_{NN}} = 2.76$ TeV. In this report, we discuss the capability of LHC experiments for heavy ion collisions, and make a short review of the recent results. Section 2 gives a brief introduction to heavy-ion collisions, and in section 3 we discuss about the experiments. In section 4, we discuss freeze-out conditions and global properties in terms of multiplicity and pseudorapidity distributions, size of the fireball, elliptic and radial flow, and fluctuations and correlations. The results on quarkonia and heavy flavour are given in section 5, section 6 discusses electroweak probes and in section 7 we give the hard probes of hot and dense matter. We conclude with a status summary and a future outlook.

2. Probing the hot and dense matter

Knowledge of the space-time evolution of the system produced in high energy heavy ion collisions provides insight into the dynamics of nuclear matter under extreme conditions. Schematic of the time evolution in case of collision of two Lorentz contracted nuclei at very high energy is shown in Fig. 1. As the colliding nuclei recede from each other, a large amount of energy is deposited in a small region of space and in a short duration of time. The matter thus created may have very high energy density and temperature, sufficient to form a baryon free region of QGP. The hot and dense plasma may not be initially in thermal equilibrium. Subsequently thermal equilibrium might set in after which the evolution may be governed by the laws of thermodynamics. As the plasma expands and cools, hadronization takes place and after some time the interactions sieze (freeze-out). Various stages during the collision can be probed by different observables, such as:

- **Freeze-out conditions and global properties:** Majority of the produced particles in the high energy nuclear collisions are emitted at freeze-out. A detailed study of these particles is crucial to estimate the energy density, pressure, entropy (s) as a function of the temperature (T) and baryon chemical potential (μ_B). These quantities may be derived from measurements of multiplicity and rapidity distributions, p_t (transverse momentum) distributions and transverse energy density (dE_T/dy). Particle flow and azimuthal asymmetry, size of the fireball from intensity

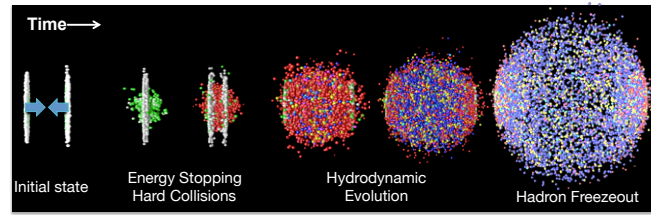


Figure 1. The time evolution of a high energy heavy ion collision.

interferometry, correlations and fluctuations, resonance production, particle ratios, etc. provide crucial information about the thermodynamics of the system.

- **Electromagnetic probes:** The electromagnetic probes, i.e. photons and dileptons are produced at different phases of evolution. They are not distorted by final state interactions and once produced can escape the interaction region, unaffected, carrying to the detectors information about the conditions and properties of the medium at the time of their production. The measurement of direct thermal radiation can be used as a direct fingerprint of the hot and dense medium.
- **Quarkonia and heavy flavour:** Quarkonia (J/ψ , ψ' , χ_c and Υ family) production is considered to provide an unique signature of QGP [1]. It is a sensitive probe of the hot and dense matter and of the gluon distributions and their modifications in nuclei. The suppression of J/ψ production has long been predicted as an important probe of a QGP formation [1], which occurs because a $c\bar{c}$ pair formed by fusion of two gluons from the colliding nuclei cannot effectively bind inside the QGP because of Debye screening. Excited states of the $c\bar{c}$ system, such as ψ' are more easily dissociated and should be largely suppressed. For the heavier $\Upsilon(b\bar{b})$ shorter screening lengths are required than for the charmonium states. Heavy flavor production, open and hidden, is considered among the most important probes for study of QCD properties of the QGP.
- **Electroweak probes:** With the increase of center-of-mass energy at the LHC, electroweak boson measurements are possible for the first time in heavy ion collisions. The lifetimes of W and Z bosons are quite short and they decay within the medium, and go unaffected through the hot and dense matter. Since leptons lose negligible energy in the medium, be it partonic or hadronic, the leptonic decay channels of W and Z may provide information about the initial state in heavy ion collisions.
- **Hard probes:** The availability of large amount of energy in the very early part of the collision gives rise to a subset of high transverse momentum processes which take place independent of the bulk, with the outgoing partons subsequently propagating through the bulk medium. Jet quenching and energy loss of high p_t hadrons constitute the most important hard probes, which play important role in determining the properties of hot and dense QCD matter.

3. LHC and its experiments

The accelerator complex at CERN is a succession of particle accelerators that can reach increasingly higher energies, starting with the duoplasmatron source for the protons and

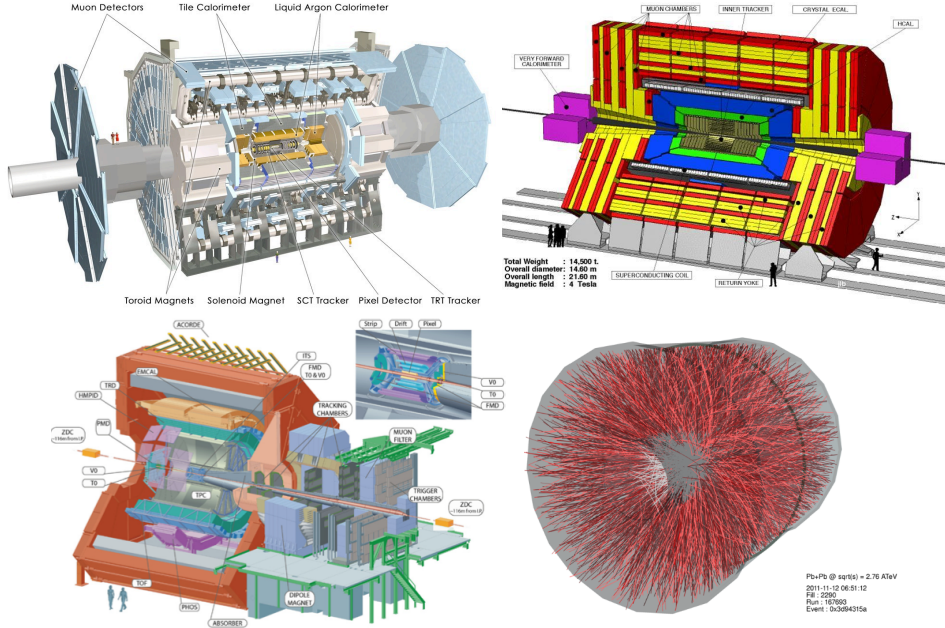


Figure 2. Schematic diagram of the ATLAS (top-left), CMS (top-right) and ALICE (bottom-left) detectors, and an event display (bottom-right) for the Pb-Pb collisions at $\sqrt{s_{NN}} = 2.76$ TeV in ALICE.

ECR ion source for the ions, and ending up at the LHC. The ions from the source are injected into a linear accelerator (LINAC3) and to the Low Energy Ion Ring (LEIR). After that the ions pass through the PS booster, then the Proton Synchrotron (PS), followed by the Super Proton Synchrotron (SPS) and finally to the LHC. For Pb-Pb collisions, a peak luminosity of $L_0 = 10^{27} \text{cm}^{-2} \text{s}^{-1}$ at $\sqrt{s_{NN}} = 5.5$ TeV has been kept as a final goal. For the first year, LHC delivered Pb-Pb collisions at $\sqrt{s_{NN}} = 2.76$ TeV with peak luminosity reaching to $L_0 = 2 \times 10^{25} \text{cm}^{-2} \text{s}^{-1}$. In addition to Pb-Pb, LHC is capable of providing collisions of other species such as Ar-Ar and asymmetric systems of p-Pb.

Sketches of the three experiments, ALICE, ATLAS and CMS are shown in Fig. 2. An event display of charge particle tracks in the ALICE experiment obtained for one of the Pb-Pb events is also shown in the figure.

The ALICE experiment [3] is specifically designed for heavy ion collisions. The low material budget and low magnetic field of the central barrel makes the experiment sensitive to low- p_t particles. The central barrel provides powerful tracking with excellent momentum resolutions, particle identification and capability for measuring high energy jets. The forward region is equipped with a muon arm, forward charged particle multiplicity detector (FMD) and photon multiplicity detector (PMD). The zero degree calorimeter and a set of scintillator detectors (Vzero, T0 and Acorde) provide timing and used in trigger.

Both the ATLAS [4] and CMS [5] detectors incorporate a broad suite of high precision subsystems which were originally optimized for very high energy p-p collisions, but also provide capabilities for studying nuclear collisions. The large acceptances of both the experiments allow for detailed study of several observables, and in particular high p_t jets.

4. Freeze-out conditions and global properties

To start with, we first discuss centrality selection in heavy ion collisions. Freeze-out conditions, global properties and many other quantities are best expressed in terms of collision centrality, which is the overlap of the two colliding nuclei. Theoretically, the collision centrality is defined in terms of impact parameter (which is the perpendicular distance between the centers of the two colliding nuclei) and essentially indicates the number of participating nucleons (N_{part}). Experimentally, several measured quantities scale with the centrality, and may be used as centrality estimators. For example, in the ALICE experiment the centrality is expressed in terms of the distribution of VZERO amplitude as shown in the left panel of Fig. 3. The peak on the left corresponds to most peripheral collisions, the plateau to the mid-central and the edge to the central collisions. The centrality resolution is an indicator for how well the centrality is known. Fig. 3 (right) gives the resolutions for different centrality estimators. The centrality resolution ranges from 0.5% in central to 2% for peripheral collisions.

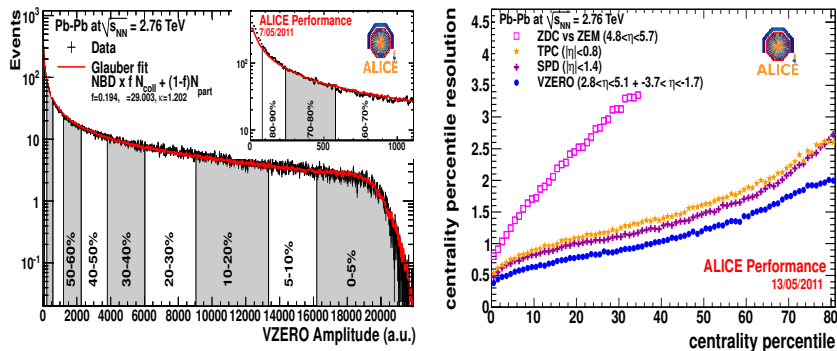


Figure 3. Left panel shows the centrality selection in ALICE and the right panel gives the centrality resolution for all centralities [6].

The collision centrality in ATLAS is estimated using the total transverse energy measured in the Forward Calorimeter (FCal, covering $3.2 < |\eta| < 4.9$). The collision centrality in CMS is determined using the total sum of transverse energy in reconstructed towers from both positive and negative fiber calorimeters (HF) covering $2.9 < |\eta| < 5.2$. In many cases, centrality for specific event classes may also be expressed as a percentage of the inelastic nucleus-nucleus interaction cross section. Below we discuss some of the global observables from the first LHC heavy ion data.

4.1 Particle multiplicities

Results on charged particle multiplicity measurements were much awaited and were the first ones to be available from the LHC heavy ion run [7]. The value of charged particle multiplicity density ($dN_{\text{ch}}/d\eta$) at central rapidity for Pb-Pb collisions at $\sqrt{s_{NN}} = 2.76$ TeV has been measured to be ~ 1600 for central collisions (0-5%). This is shown in the left panel of Fig. 4. Also shown are recent predictions from various models. As we see, the experimental result is on the higher side of most of the predicted values. The rapidity distributions of the charged particle multiplicity density per participant pair have

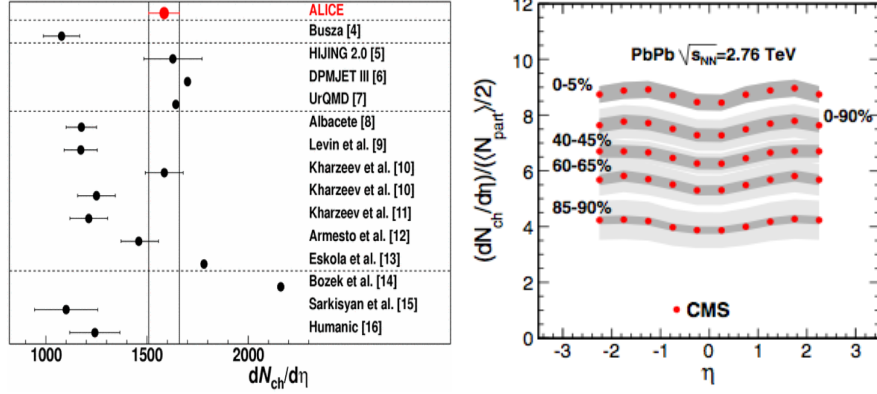


Figure 4. Left panel shows the pseudorapidity multiplicity distribution at mid rapidity compared to various model predictions [7]. The right panel shows charged particle multiplicity density per participant pair for different centralities as a function of η [8].

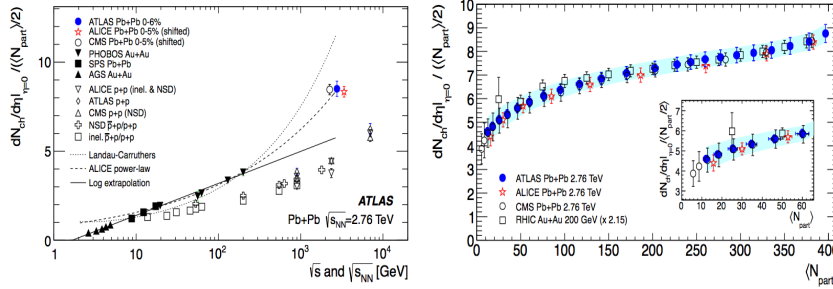


Figure 5. Left panel shows the energy dependence of charged particle pseudorapidity density, $dN_{ch}/d\eta$ per colliding nucleon pair ($0.5N_{part}$) for pp (or p \bar{p} and AA collisions). The right panel shows the centrality dependence of $dN_{ch}/d\eta$ per participant pair [9].

been measured by the CMS experiment [8] and shown in the right panel of Fig. 4 for peripheral (85-90%) to central (0-5%) collisions.

Energy dependence of charge particle multiplicity density has been compiled by combining the results from all three LHC experiments along with those from RHIC, SPS and AGS. This is shown in the left panel of Fig. 5 for central collisions. The results for corresponding p-p collisions for NSD processes are also superimposed in the figure. We note here two interesting facts: (1) the energy dependence is steeper for heavy ion collisions than for p-p collisions, and (2) a significant increase in the pseudorapidity density at LHC compared to extrapolations from lower energies.

The right panel of Fig. 5 shows centrality dependence of charged particle multiplicity density per participant pair obtained by all three LHC experiments along with the scaled value for Au-Au collisions at RHIC top energy. A moderate variation [9] is observed, from a value of 4.6 for peripheral collisions to 8.8 for central collisions. The RHIC data, scaled by a factor of 2.15 are seen to match well with those of the LHC results.

Heavy Ions: Results from the LHC

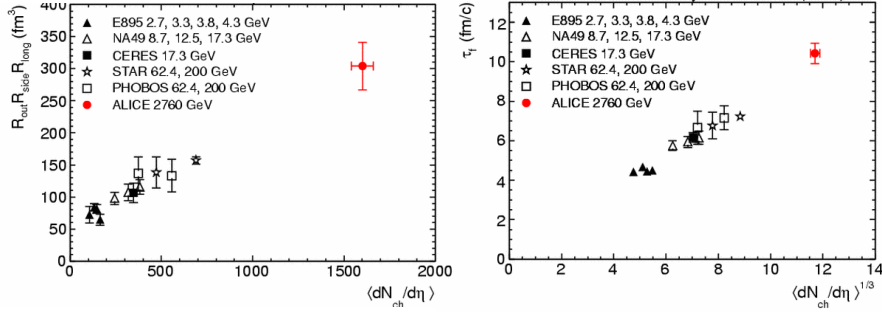


Figure 6. Left Panel shows the local freeze-out volume measured by identical pion interferometry as a function of pseudo-rapidity density of charged particles from AGS, SPS, RHIC and LHC energies [10]. The right panel shows the system lifetime (τ_f) for these energies [10]

4.2 Size of the fireball and lifetime

The information about the freeze-out volume and lifetime of the created system in p-p and heavy ion collisions from the measured particle momenta have been extracted [10] by using the method of Bose-Einstein correlations or the Hanbury-Brown and Twiss (HBT) technique. All the three pion source radii, longitudinal (R_{long}), outward (R_{out}), and side-ward (R_{side}) are observed to grow compared to those of the results from RHIC. Fig 6 shows the product of the three radii as a function of charged particle multiplicity density for central collisions at LHC, RHIC and SPS energies. The homogeneity volume is observed to be larger by a factor of two at LHC compared to RHIC [11].

or the decoupling time (τ_f), which is the time between collision and freeze-out for hadrons at mid-rapidity, has been estimated [10] from $R_{\text{long}}(k_T)$ by using the expressions:

$$R_{\text{long}}^2(k_T) = \frac{\tau_f^2 T}{m_T} \frac{K_2(m_T/T)}{K_1(m_T/T)}, \quad (1)$$

where m_T is the pion mass, T is the kinetic freeze-out temperature (~ 0.12 GeV) and K_1 and K_2 are the integer order modified Bessel functions. The decoupling times, shown in Fig. 6, are seen to be The decoupling time for mid-rapidity pions, as shown in Fig. 6 are seen to exceed 10 fm/c which is 40% larger than at RHIC.

4.3 Anisotropic flow

Anisotropic flow measurement in nuclear collisions provides one of the most important measures of the collective dynamics of the system [12–14]. The magnitude of the anisotropic flow depends strongly on the friction in the created matter, characterized by the shear viscosity over entropy density ratio (η/s). The large elliptic flow observed at RHIC provided compelling evidence for strongly interacting matter which, in addition, appears to behave like an almost perfect fluid [15].

The left panel of Fig. 7 shows the integrated elliptic flow measured in the 20-30% centrality class, plotted for LHC energy along with results from RHIC and lower energies. An increase in the magnitude ($\sim 30\%$) of v_2 at LHC has been observed compared to the results at RHIC top energy. This increase may be the result of the increase in the average

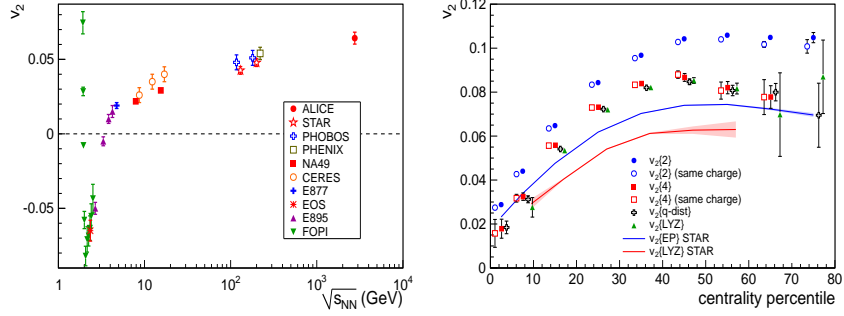


Figure 7. Integrated elliptic flow (v_2) a function of collision energy for non-central collisions (left) and as a function of centrality going from central to peripheral collisions (right) [12].

transverse momentum at LHC compared to RHIC. The right panel of Fig. 7 shows the centrality dependence of elliptic flow (v_2) for Pb-Pb collisions at $\sqrt{s_{NN}} = 2.76$ TeV. The integrated elliptic flow increases from central to peripheral collisions and reaches a maximum value in the 50-60% and 40-50% centrality classes. These results are consistent with hydrodynamic model calculations.

4.4 Fluctuations and correlations

Event-by-event studies of fluctuations and correlations provide direct evidence for the QGP formation and of the thermalized system formed in heavy ion collisions. The order of phase transition may also be inferred from these studies. At the LHC, the first such studies have been performed for net-charge and mean- p_t fluctuations.

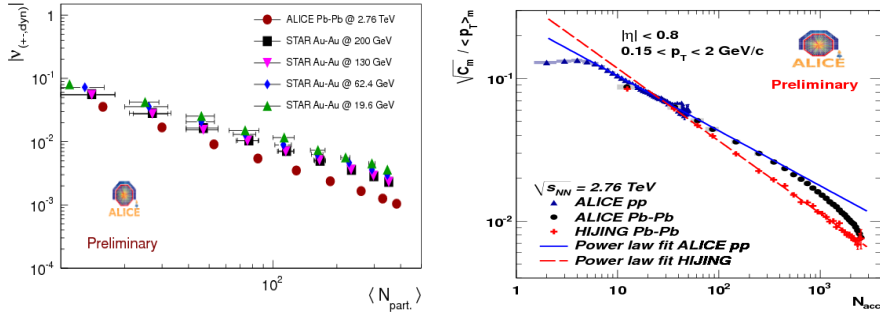


Figure 8. (Left) Dynamical net-charge fluctuations, $\nu_{(+-,dyn)}$, of charged particles as a function of centrality, expressed by the number of participating nucleons, for Pb-Pb (right) events at $\sqrt{s_{NN}} = 2.76$ TeV, along with data from RHIC [18]. (Right) The dependence of the relative mean p_t fluctuations on the number of accepted tracks in Pb-Pb collisions, compared to different model predictions [19, 20].

The fluctuations of net-charge (difference of +ve to -ve charge multiplicities) depend on the squares of the charge states present in the system. Fluctuations in a QGP phase having quarks (with fractional charges) as the charge carriers are significantly different from those of a hadron gas (with unit charges). Net-charge fluctuations may be expressed

by the quantity, $D = 4 \frac{\langle \delta Q^2 \rangle}{N_{\text{ch}}}$, where $\langle \delta Q^2 \rangle$ is the variance of the net-charge Q with $Q = N_+ - N_-$ and $N_{\text{ch}} = N_+ + N_-$. Here N_+ and N_- are the numbers of positive and negative particles. Typical values of D are close to 1 for a QGP and 3 for a hadron gas [16]. Thus a measured value of D will be able to indicate whether the particles originate from a QGP or from hadron gas. Experimentally the dynamic fluctuations in net-charge may be expressed in terms of $\nu_{(+-, \text{dyn.})}$ [17], which is related to D . The left panel of Fig. 8 gives the centrality dependence of the absolute value of $\nu_{(+-, \text{dyn.})}$ in a log-log scale. The measurements at LHC are compared to the corresponding measurements [18] at RHIC, which show an additional reduction of the magnitude of fluctuations at LHC.

The mean transverse momentum $\langle p_t \rangle$ of emitted particles in an event is correlated to the temperature associated with the p_t distribution and thus to the transverse collective expansion of the colliding system. The study of the $\langle p_t \rangle$ fluctuations can probe the dynamics and the underlying correlations of the created system. A two particle correlator, $C_m = \langle \Delta p_{t,i}, \Delta p_{t,j} \rangle_m$ is used which comprises of the dynamical component of the relevant fluctuations. The relative fluctuation expressed as $\sqrt{C_m} / \langle p_t \rangle_m$, is shown in the right panel of Fig. 8 for Pb-Pb collisions at $\sqrt{s_{NN}} = 2.76$ TeV as a function of number of accepted tracks (N_{acc}). Compared to the p-p reference, the data points for central collisions (higher N_{acc}) show reduction of fluctuations.

5. Quarkonia and heavy flavour

Comparison of the suppression pattern of quarkonia (flavourless mesons whose constituents are a quark and its own anti-quark) in nuclear collisions to those of the p-p collisions and the study of heavy-flavour particles which are abundantly produced at LHC energies, provide detailed information about the early conditions of the produced fireball.

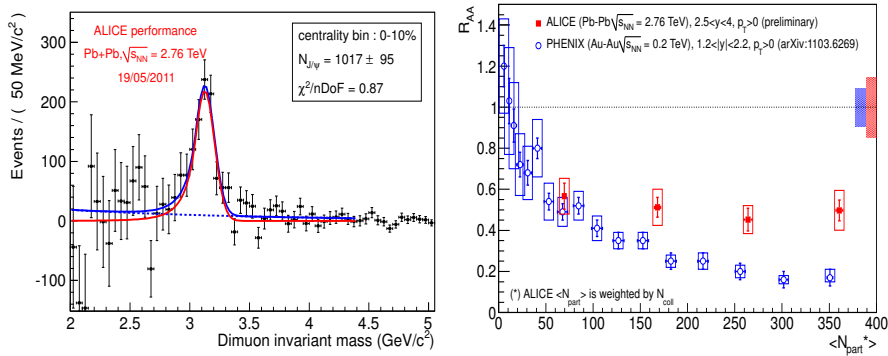


Figure 9. Left panel shows the background subtracted invariant mass distribution for opposite-sign muon pairs in the centrality class 0-10%, showing the J/ψ peak. The right panel shows R_{AA} of J/ψ as a function of number of participants for LHC data compared to those of the data from RHIC. Figures are taken from [21, 22].

Opposite sign dimuon invariant mass distribution, after the subtraction of the combinatorial background using the event-mixing technique shows the J/ψ peak as depicted in the left panel of Fig. 9. The nuclear modification of factor R_{AA} which gives the deviation in J/ψ yields from A-A collisions related to the scaled yields of J/ψ from p-p collisions, is shown in the right panel of figure. The R_{AA} is seen to be about 0.5 and independent of centrality. The suppression of J/ψ is seen to be about factor 2 less at LHC compared to

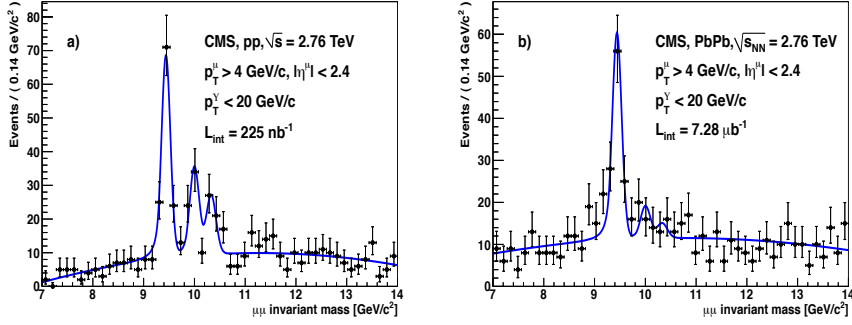


Figure 10. Dimuon invariant-mass distributions in the Υ region [23] for p-p (left panel) and Pb-Pb (right panel) collisions. The solid lines are fits to extract the yields.

the results at RHIC from PHENIX experiment. On the other hand, the ATLAS and CMS results [23] show that J/ψ is strongly suppressed at high p_t , and similar to the PHENIX data at RHIC. In order to understand the suppression and regeneration effects, a better knowledge of the cold nuclear matter effects is required. For this reason a pPb run, which will address these nuclear effects, is being planned in the year 2012.

First measurements of Υ production with p-p and PbPb collisions at LHC [23] are made and shown in Fig. 10. The higher state contribution relative to the ground state is strikingly smaller in Pb-Pb collisions compared to the p-p collisions. Even with the large statistical errors, we can conclude that the excited, higher mass Υ states are more suppressed than the tightly bound ground state $\Upsilon(1S)$, as expected in a deconfinement scenario.

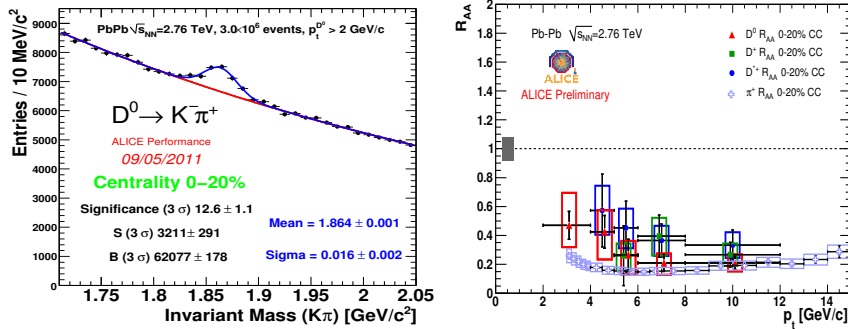


Figure 11. (Left) $K\pi$ invariant mass showing the $D^0 \rightarrow K^-\pi^+$ signal for central (020%) PbPb collision, and (Right) R_{AA} for D_0 , D_+ and π^+ in central collisions [24].

Heavy-flavours such as D mesons are sensitive to energy density. Their detection strategy at central rapidity is based on the selection of displaced-vertex topologies, i.e. separation of tracks from the secondary vertex from those from the primary vertex, large decay length and good alignment between the reconstructed D meson momentum and flight-line. An invariant-mass analysis is then used to extract the raw signal yield. Corrections are made for detector acceptance and PID, selection and reconstruction efficiencies.

Heavy Ions: Results from the LHC

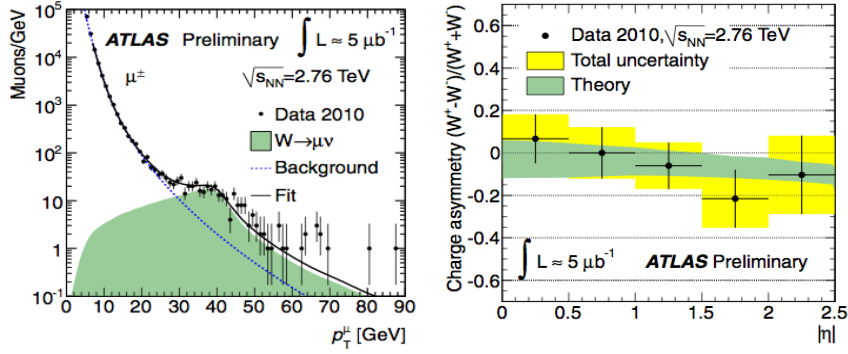


Figure 12. (Left) Extraction of the number of $W \rightarrow \mu\nu$ events from the uncorrected inclusive muon p_t spectrum in Pb-Pb collisions at $\sqrt{s_{NN}} = 2.76$ TeV. (Right) Muon charge asymmetry from W^\pm decays. [25].

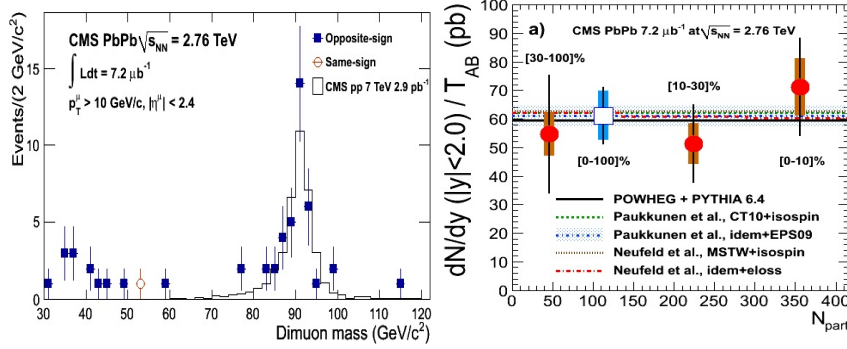


Figure 13. (Left) Dimuon invariant mass showing a clear peak around Z boson mass in Pb-Pb collisions at $\sqrt{s_{NN}} = 2.76$ TeV. (Right) Z differential yield divided by the nuclear overlap function as a function of number of participating nucleons. [26].

The $D^0 \rightarrow K^- \pi^+$ signal was measured in five p_t bins in 2-12 GeV/ c and the $D^+ \rightarrow K^- \pi^+ \pi^+$ signal in three bins in 5-12 GeV/ c . An example $K\pi$ invariant mass distribution for $p_t > 2$ GeV/ c in the 0-20% centrality class is shown in the left panel of Fig. 11. A clear peak at the D^0 mass is seen. The nuclear modification factor (R_{AA}) of prompt D^0 and D^+ mesons in central (0-20%) PbPb collisions is shown in the right panel of Fig. 11. A strong suppression is observed, reaching a factor 4 to 5 for $p_t > 5$ GeV/ c for both D meson species. For comparison, the values for charged pions is superimposed in the figure. The suppression for D mesons is comparable with that of the charged pions.

6. Electroweak Probes

The ATLAS and CMS experiments have measured the W and Z production in the heavy ion collisions at the LHC [25, 26]. ATLAS studies the production of W bosons via the measurement of the inclusive muon p_t spectrum as shown in the left panel of Fig. 12. The spectrum is fitted (solid line) with two components: signal $W \rightarrow \mu\nu$ (shaded area) and a background parametrization (dashed line). The amplitude of W -decay curve gives the

number of W events on the data. Similar studies are also reported by the CMS experiment. A precision measurement of the W boson production charge asymmetry can provide a test of PDF (parton distribution function), which may lead to the understanding of possible modifications to the PDF due to nuclear effects. The muon charge asymmetry is shown in the right panel of Fig. 12 for different η -window. Although the statistical errors are dominating, one may conclude that production cross section for W^- and W^+ is similar.

Among the leptonic decays of the electroweak bosons, the study of the Z boson in the $\mu^+\mu^-$ channel is the cleanest one [26]. The reconstruction of the Z boson in the dimuon channel is done by requiring two opposite-charge muons, each with $p_t^\mu > 10$ GeV/c and $|\eta_\mu| < 2.4$. A clear peak in the 60-120 GeV/ c^2 mass region is observed as shown in the invariant mass spectrum in the left panel of Fig. 13. Differential yields divided by the nuclear overlap function is plotted in the right panel of the figure, which shows that the distribution is flat (within uncertainty) as a function of centrality.

7. Hard probes

Hard processes, where we study the higher side of the p_t spectrum, provides a means to probe the conditions of the collision at very early times. This is typically done by means of suppression observables such as R_{AA} which indicate deviations from the expected scaling of yields by the number of binary collisions, estimated using the Glauber model, and by the study of jets quenching. Suppression of high p_t hadron yields result from energy loss suffered by hard-scattered partons passing through the medium. The parton energy loss provides fundamental information on the thermodynamical and transport properties of the traversed medium. Below we discuss the current LHC results on these aspects.

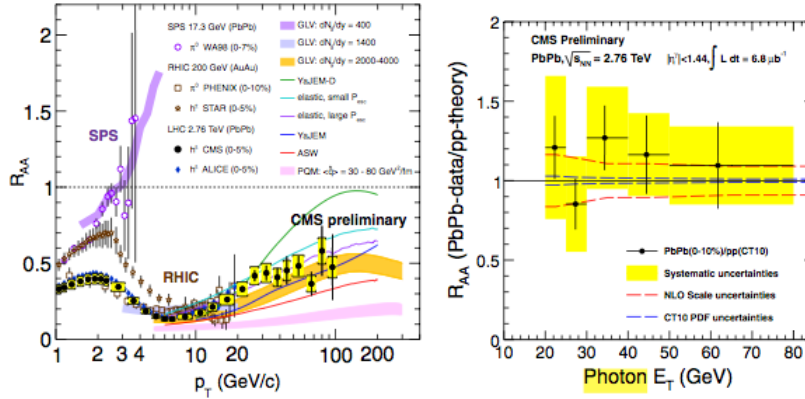


Figure 14. (Left) R_{AA} as a function of p_t for neutral pions and charged hadrons in central heavy-ion collisions at SPS, RHIC and LHC energies. (Right) R_{AA} of isolated photons as a function of p_t for central events at LHC [8].

7.1 R_{AA} of Charged particle and photons

The nuclear modification factor, R_{AA} , which gives the modification of the charged particle p_t spectrum, compared to nucleon–nucleon collisions at the same energy, can shed light on the detailed mechanism by which hard partons lose energy traversing the medium.

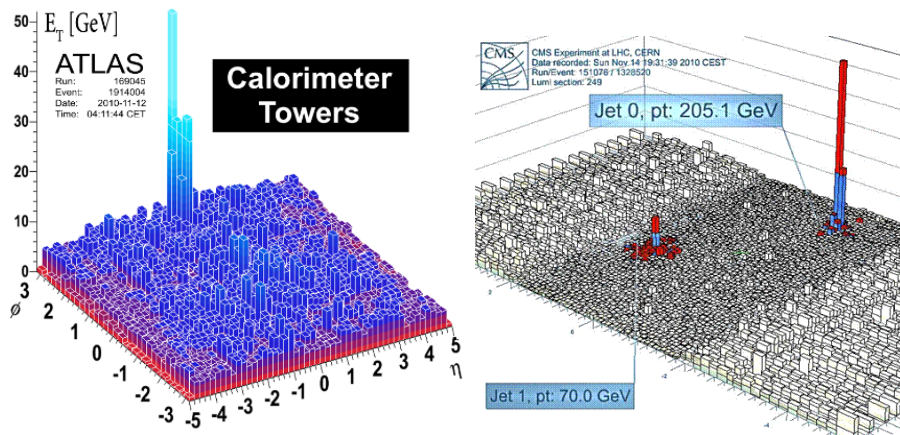


Figure 15. Examples of unbalanced dijet events in PbPb collisions at $\sqrt{s_{NN}} = 2.76$ TeV. Figures are taken from [27] and [28].

R_{AA} has been measured in CMS for all charged particles with p_t up to 100 GeV/c. The ratio is plotted in the left panel of Fig. 14 and compared to theoretical predictions. A stronger suppression compared to those of the RHIC data has been observed.

Direct photon production as a function of centrality and p_t has been made by the CMS experiment [8]. The ratio, R_{AA} as a function of photon p_t is shown in the right panel of Fig. 14. The results are compared to the NLO pQCD predictions. Within statistical uncertainties, the direct photons are seen to be not suppressed compared to p-p collisions.

7.2 Jet quenching and dijet asymmetry

At the LHC, very high p_t jets are most of the time easily visible above the soft background [27, 28] because of the availability of large energy. The medium effects are studied by analyzing the transverse energy of dijets in opposite hemispheres. Fig. 15 shows typical events in both ATLAS and CMS experiments with large imbalance in energy from one of the hemisphere to the other. This is a very striking observation and direct evidence of jet quenching. The transverse energies of dijets in opposite hemispheres is observed to become systematically more unbalanced with increasing event centrality leading to a large number of events which contain highly asymmetric dijets. One of the main question is to find out what happened to the energy in the opposite hemisphere.

Quantitative measurements of dijet asymmetry have been reported by both ATLAS [27] and CMS [28] experiments. The upper panel of Fig. 16 shows the dijet asymmetry for peripheral to central collisions. Proton-proton data from $\sqrt{s} = 7$ TeV, analyzed with the same jet selection, is shown as open circles, whereas the solid histograms depict the results from PYTHIA dijet simulations. For p-p and for peripheral collisions, the asymmetry value is peaked at or close to zero, implying the jets are balanced on both hemispheres. For central collisions, a marked asymmetry develops with unbalanced jets ($A_j > 0$). This shows an enhancement of events with large dijet asymmetries, not observed in p-p collisions. The bottom panels of Fig. 16 shows the CMS results on the azimuthal angle between the dijets for p-p and for different centrality ranges in Pb-Pb. In all cases, the two jets stay mostly back-to-back in azimuth. CMS has also measured the distribution of energy around the jets with most of the lost energy appearing in very low momentum

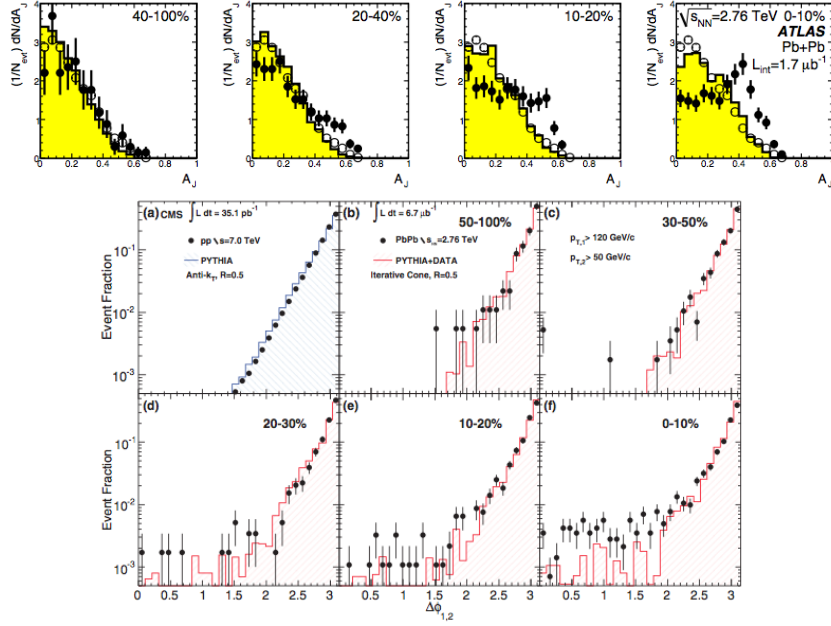


Figure 16. (Top) Dijet asymmetry for different centrality bins for Pb-Pb collisions, showing a strong centrality dependence. (Below) Azimuthal angle distributions between dijets for different centrality bins [27] and [28].

fragments far away from the jet direction [28]. Results from both ATLAS and CMS point to jet quenching and an interesting new mechanism where the energy is radiated away via multiple, soft gluons, which in turn may even re-interact in the medium and lead to a further degradation of the energy.

8. Summary and outlook

With the acceleration of heavy ions in the year 2010, the LHC has entered a new domain of physics. The first data, recorded and analyzed by ALICE, ATLAS and CMS experiments have been most impressive in terms of the results, some of which are consistent with present understandings and some others which are not. The salient features of the latest findings are as follows:

- The results of the multiplicity distributions, fluctuations and Bose-Einstein correlations point to the formation of a fireball which is hotter, long lived and larger in size, much more than those measured at RHIC.
- Measurements of anisotropic flow infer to the formation of a system which behaves like an almost perfect fluid with almost no friction. This will provide strong constraints on the temperature dependence of η/s .
- The J/ψ suppression is found to be similar in magnitude to SPS and RHIC. One of the possible explanations of this observation is that the suppression of J/ψ may be getting balanced by coalescence of two independently created charm quarks. Detailed measurement of both J/ψ and Υ families will be needed to answer this.

Heavy Ions: Results from the LHC

- In central collisions, a large suppression of heavy flavours is observed, indicating that charm quarks undergo a strong energy loss in the hot and dense matter.
- Electroweak W and Z boson measurements have become possible for the first time in heavy ion collisions. These channels may indeed provide most sensitive probes of the initial state of QGP matter.
- Unexpectedly large dijet asymmetry and strong jet energy loss have been observed, suggesting strong interactions between jets and a hot, dense medium.

The available results take us one step closer to understanding the primordial state of matter that existed within few microseconds after the Big Bang. Better understanding is expected in near future with more exclusive measurements and more theoretical studies.

Acknowledgement: We would like to thank the Organizers of Lepton-Photon 2011 for the invitation to present LHC heavy ion results. We would like to thank the LHC Operations for providing excellent beams, and to the members of ALICE, ATLAS and CMS Collaborations for the analysis results. In particular, we would like to express our thanks to Panos Christakoglou, Premomoy Ghosh, Paolo Giubellino, Satyajit Jena, Sanjib Muhuri, Peter Steinberg, Ermanno Vercelli, and Bolek Wyslouch for their help during preparation of the talk and the manuscript.

References

- [1] H. Satz, Nucl. Phys. **A862**, (2011) 4.
- [2] J. Kapusta, Nucl. Phys. **A862**, (2011) 47.
- [3] K. Aamodt *et al.* (ALICE Collaboration), JINST **3**, (2008) S08002.
- [4] G. Aad *et al.* (ATLAS Collaboration), JINST **3**, (2008) S08003.
- [5] R. Adolphi *et al.* (CMS Collaboration), JINST **3**, (2008) S08004.
- [6] K. Aamodt *et al.* (ALICE Collaboration) Phys. Rev. Lett. **106**, (2011) 032301.
- [7] K. Aamodt *et al.* (ALICE Collaboration) Phys. Rev. Lett. **105** (2010) 252301 (2010).
- [8] B. Wyslouch *et al.* (CMS Collaboration) J. Phys. G: Nucl. Part. Phys. **38** (2011) 124005.
- [9] G. Aad *et al.* (ATLAS Collaboration), [arXiv:1108.6027 [hep-ex]].
- [10] K. Aamodt *et al.* (ALICE Collaboration) Phys. Lett. **B696** (2011) 328.
- [11] B.I. Abelev *et al.* (STAR Collaboration) Phys. Rev. **C80** (2009) 024905.
- [12] K. Aamodt *et al.* (ALICE Collaboration) Phys. Rev. Lett. **105** (2010) 252302.
- [13] R. Snellings *et al.* (ALICE Collaboration) J. Phys. G: Nucl. Part. Phys. **38** (2011) 124013.
- [14] J. Schukraft, arXiv:1112.0550v1 [hep-ex].
- [15] P. Kovtun, D. T. Son, A. O. Starinets, Phys. Rev. Lett. **94** (2005) 111601.
- [16] S. Jeon, V. Koch, Phys. Rev. Lett. **85**, (2000) 2076.
- [17] C. Pruneau, S. Gavin and S. Voloshin, Phys. Rev. **C 66** (2002) 044904.
- [18] B. I. Abelev *et al.* (STAR Collaboration), Phys. Rev. **C79**, (2009) 024906.
- [19] P. Christakoglou *et al.* (ALICE Collaboration), arXiv:1111.4506v1 [nucl-ex].
- [20] S. Jena *et al.* (ALICE Collaboration), arXiv:1201.0130 [hep-ex].
- [21] P. Pillot *et al.*) (ALICE Collaboration) J. Phys. **G38** (2011) 124111.
- [22] D. Das *et al.*) (ALICE Collaboration) arXiv:1111.5946v1 [nucl-ex].
- [23] S. Chatrchyan *et al.* (CMS Collaboration), Phys. Rev. Lett. **107** (2011) 052302.
- [24] A. Dainese *et al.* (ALICE Collaboration) J. Phys. G: Nucl. Part. Phys. **38** (2011) 124032.
- [25] R Sandstrm *et al.* (ATLAS Collaboration) J. Phys. G: Nucl. Part. Phys. **38** (2011) 124133.
- [26] S. Chatrchyan *et al.* (CMS Collaboration), Phys. Rev. Lett. **106** (2011) 212301.
- [27] G. Aad *et al.* (ATLAS Collaboration) Phys. Rev. Lett. **105** (2010) 252303.
- [28] S. Chatrchyan *et al.* (CMS Collaboration) Phys. Rev. **C84** (2011) 024906.